

# Design of Aircraft Trajectories based on Trade-offs between Emission Sources

Banavar Sridhar and Neil Y. Chen  
NASA Ames Research Center  
Moffett Field, CA, USA

Hok K. Ng  
University of California  
Santa Cruz, CA, USA

Florian Linke  
DLR-German Aerospace Center  
Hamburg, Germany

**Abstract** – Aviation operations affect the climate in several ways. Carbon dioxide, water vapor and other greenhouse gasses are unavoidable by-product of the combustion of fossil fuel. There are indications that persistent contrails can lead to adverse climate change, although the complete effect on climate forcing is still uncertain. A flight trajectory optimization algorithm with fuel and contrails models, which develops alternative flight paths, provides policy makers the necessary data to make trade-offs between persistent contrails mitigation and aircraft fuel consumption. This study develops an algorithm that calculates wind-optimal trajectories for cruising aircraft while reducing the amount of time spent in regions of airspace prone to persistent contrails formation. The optimal trajectories are developed by solving a non-linear optimal control problem with path constraints. The regions of airspace favorable to persistent contrails formation are modeled as penalty areas that aircraft should avoid. The trade-off between persistent contrails formation and additional fuel consumption is investigated for 12 city-pairs in the continental United States. The avoidance of contrails using only horizontal maneuvers results in a small reduction of contrails with increasing fuel consumption. When both horizontal maneuvers and altitude are optimized, a 2% increase in total fuel consumption can reduce the total travel times through contrail regions by more than 70%. Allowing further increase in fuel consumption does not seem to result in proportionate reduction in contrail travel times. This trend is maintained even in the presence of uncertainties in the contrail formation regions such as uncertainties in relative humidity values computed by weather forecast models.

**Keywords** – Trajectory Optimization, Contrails Avoidance, Aircraft Emissions, Climate Impact

## I. INTRODUCTION

Aviation is responsible for 2% of all man-made carbon-dioxide ( $\text{CO}_2$ ) emissions. Aircraft engines combine air and fuel to provide the thrust to propel the aircraft. The oxygen and nitrogen in the air together with the hydrocarbons and sulfur in the aviation fuel

results in byproducts of combustion, which includes  $\text{CO}_2$ , water vapor ( $\text{H}_2\text{O}$ ), oxides of nitrogen ( $\text{NO}_x$ ), oxides of sulfur ( $\text{SO}_x$ ), hydrocarbons and soot. The byproducts and their effect on the climate are illustrated in Fig. 1.  $\text{CO}_2$  and water vapor directly affect the climate through their direct absorption and re-emission of infrared radiation.  $\text{NO}_x$  is converted in the atmosphere by chemical reactions to methane ( $\text{CH}_4$ ) and ozone ( $\text{O}_3$ ). Water vapor emission reduces  $\text{O}_3$ , whereas  $\text{NO}_x$  increases it. Ozone affects the radiative balance through the absorption shortwave and infrared radiation.  $\text{NO}_x$  emissions from the aircraft result in the reduction of methane in the atmosphere. The release of these products into the atmosphere causes a change in the amount of radiative force (RF) from these components resulting in climate change as measured in variations to the temperature, mean sea level, rainfall and other indicators.

Interest in the effect of aircraft condensation trails or contrails on climate change has increased in recent years. Contrails form in the wake of aircraft for various reasons but the most important is the emission of water vapor<sup>1</sup>. They appear in the atmosphere along the aircraft's trajectory at high altitude where the ambient temperature is very low. Contrails persist in the region of atmosphere where the relative humidity with respect to ice is greater than 100%<sup>2</sup>. Contrails can lead to the formation of cirrus clouds having a radiative impact on the climate. A recent study<sup>3</sup> reports that persistent contrails may have a three to four times greater effect on the climate than  $\text{CO}_2$  emissions. It is tempting to reroute aircraft to minimize the impact of persistent contrails on climate. This may result in longer travel times, more fuel usage and increased  $\text{CO}_2$  emissions. However, the complete effect of persistent contrails on climate change is still not known as they have both negative and positive effects and the resulting net effect is uncertain. The uncertainty in the effect of persistent contrails on climate forcing requires a flight

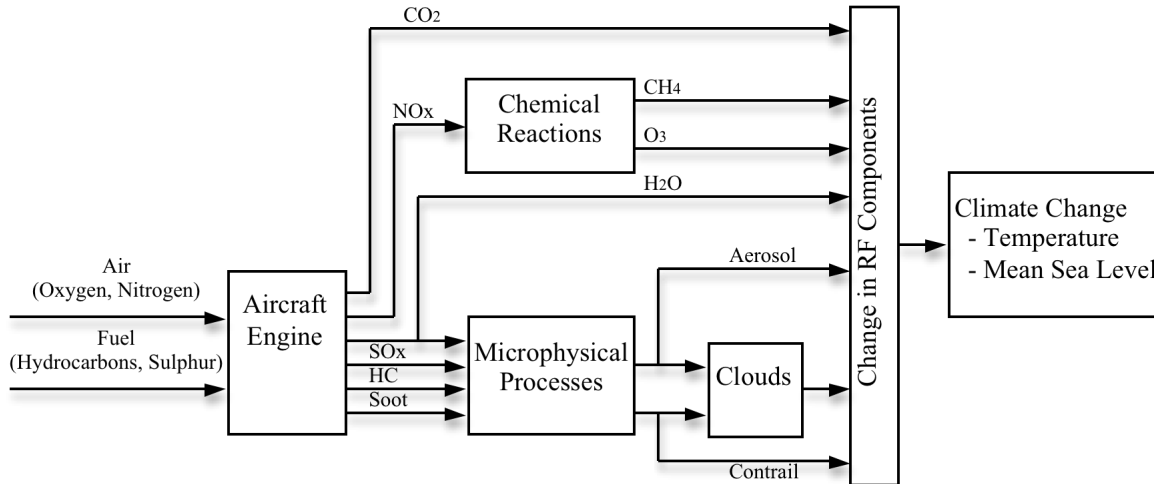


Figure 1. Aviation emissions and their impact on climate

trajectory optimization algorithm with fuel and contrails models that can develop alternative flight paths to enable trade-off between persistent contrails mitigation and fuel consumption for policy makers to set acceptable aviation operation guidelines.

Several new operational strategies in air traffic management have been proposed that can potentially mitigate the impact of persistent contrails on climate change. These strategies include adjusting cruise altitude in real-time<sup>4</sup> and rerouting aircraft around regions of airspace that facilitate persistent contrails formation<sup>5</sup>. The study in Ref. 6 presents a methodology to optimally reroute aircraft trajectories to avoid the formation of persistent contrails with the use of mixed integer programming. However, the computational complexity is high for problems with many obstacles and dynamic constraints. None of the current methods for avoiding contrails<sup>6-7</sup> consider the effect of wind on the aircraft trajectory and therefore neglect the potential fuel savings that aircraft can gain when flying wind-optimal routes.

The emphasis in this paper is on the use of actual traffic data, contrail formation based on current and forecast weather data and contrail reduction strategies in the presence of winds. This study develops an algorithm to calculate a wind-optimal trajectory for cruising aircraft while avoiding the regions of airspace that facilitate persistent contrails formation. The computationally efficient optimal trajectory is derived by solving a non-linear optimal control problem with path constraints<sup>8</sup>. The regions of airspace favorable to persistent contrails formation are modeled as undesirable regions that aircraft should avoid and are formulated as soft state constraints. It is shown that the dynamical equation for aircraft optimal heading is

reduced to the solution of the Zermelo problem<sup>9</sup> in the absence of constrained airspace regions.

Section II provides the model for diagnosing regions of airspace that are susceptible for persistent contrail formation. Section III explains the optimal trajectory generation for cruising aircraft. Section IV describes the application of the trajectory optimization algorithm for calculating wind-optimal and contrails-avoidance routes. Section V considers the impact of uncertainty in weather models on the trade-off curves. Conclusions and future work are described in Section VI.

## II. PERSISTENT CONTRAILS FORMATION MODELS

The formation of contrails has been under investigation since 1919<sup>1</sup>. According to Appleman<sup>10</sup>, contrails are clouds that form when a mixture of warm engine exhaust gases and cold ambient air reaches saturation with respect to water, forming liquid drops, which quickly freeze. Contrails form in the regions of airspace that have ambient Relative Humidity with respect to Water (RH<sub>w</sub>) greater than a critical value,  $r_{contr}$ <sup>11</sup>. Contrails can persist when the ambient air is supersaturated with respect to ice, that is the environmental Relative Humidity with respect to Ice (RH<sub>i</sub>) is greater than 100%<sup>2</sup>. In this study, the regions of airspace that have RH<sub>w</sub> greater than  $r_{contr}$  and RH<sub>i</sub> greater than 100% are considered favorable to persistent contrails formation. The studies in Refs. 12-13 measure the validity of contrails formation by comparing them with satellite observation. There is general agreement between the satellite images and the persistent contrails regions predicted by the model.

The estimated critical relative humidity  $r_{contr}$  for contrails formation at a given temperature  $T$  (in Celsius) can be calculated as<sup>11</sup>

$$r_{contr} = \frac{G(T - T_{contr}) + e_{sat}^{liq}(T_{contr})}{e_{sat}^{liq}(T)} \quad (1)$$

where  $e_{sat}^{liq}(T)$  is the saturation vapor pressure over water at a given temperature. The estimated threshold temperature (in Celsius) for contrails formation at liquid saturation is<sup>1</sup>

$$T_{contr} = -46.46 + 9.43 \ln(G - 0.053) + 0.72 \ln^2(G - 0.053) \quad (2)$$

where  $G = \frac{EI_{H_2O} C_p P}{\epsilon Q(1 - \eta)}$ .  $EI_{H_2O}$  is the emission index of water vapor, and it is assumed to be 1.25;  $C_p = 1004 \text{ JKg}^{-1} \text{ K}^{-1}$  is the isobaric heat capacity of air,  $P$  (in Pa) is the ambient air pressure,  $\epsilon = 0.6222$  is the ratio of molecular masses of water and dry air,  $Q = 43 \times 10^6 \text{ JKg}^{-1}$  is the specific combustion heat, and  $\eta = 0.3$  is the average propulsion efficiency of the jet engine.

The values of  $r_{contr}$  and RHi are computed using measurements from the Rapid Update Cycle (RUC). RUC is an operational weather prediction system developed by the National Oceanic & Atmospheric Administration (NOAA) for users needing frequently updated short-range weather forecasts (e.g. the US aviation community). The horizontal resolution in RUC is 40-km. RUC data has 37 vertical isobaric pressure levels ranging between 100-1000mb in 25mb increments. The RUC produces short-range forecasts every hour. The value of  $r_{contr}$  is computed by Eqs (1, 2) using RUC measurements for RHw and temperatures. RUC does not provide measurements for RHi directly. Instead, RHi is calculated by the following formula<sup>14</sup>:

$$RHi = RHw \cdot \frac{6.0612e^{18.102T/(249.52+T)}}{6.1162e^{22.577T/(273.78+T)}} \quad (3)$$

Note that the numerator on the right hand side of Eq. (3) is the saturation vapor pressure over water  $e_{sat}^{liq}(T)$  from the model denoted as AERW(50, -80) in Ref. 14 and the denominator is the saturation vapor pressure over ice from the model denoted as AERWi(0, -80) in Ref. 14.

### III. OPTIMAL HORIZONTAL TRAJECTORY

Aircraft trajectory optimization algorithms are well known and are solutions to two-point boundary value problems<sup>9</sup>. The various approximations to the solution

of the two-point boundary value problems depend on the application, and are motivated by the desire to balance computation speed with accuracy. The cruise altitude of most commercial aircraft varies between 29,000 feet to 41,000 feet. Eastbound aircraft fly odd thousands of feet while westbound traffic fly even thousands of feet. The flight levels are separated by 2000 feet between two levels of flight in the same direction (1000 feet since the introduction of Reduced Vertical Separation Minima). As the choice of the cruise altitude varies over a small range, the optimal aircraft trajectories in this paper are computed by repeatedly solving the horizontal plane problem.

This section develops the optimal trajectory algorithm for cruising aircraft. Section III.A presents the aircraft model and outlines the procedures for calculating optimal aircraft heading on a plane. Section III.C models persistent contrails formation as regions to be avoided by an aircraft and imposes a soft penalty for going through these regions.

#### A. Aircraft Model and Horizontal Trajectory Generation

The equations of motion in the horizontal plane are

$$\dot{x} = V \cos \theta + u(x, y) \quad (4)$$

$$\dot{y} = V \sin \theta + v(x, y) \quad (5)$$

$$\dot{m} = -f \quad (6)$$

subject to the conditions that  $Th=D$  and flight path angle,  $\gamma=0$ , where  $x$  and  $y$  are aircraft position in rectangular coordinates,  $V$  is airspeed,  $\theta$  is heading angle,  $m$  is aircraft mass,  $f$  is fuel flow rate,  $Th$  is thrust and  $D$  is drag. The x-component of the wind velocity is  $u(x, y)$ , and the y-component of the wind velocity is  $v(x, y)$ .

The horizontal trajectory is optimized by determining the heading angle that minimizes a cost function and satisfies the physical system constraints. The cost function contains components that penalize travelling time, fuel burn, and flying through penalty areas<sup>15</sup>. The cost function is defined as

$$J = \frac{1}{2} X^T(t_f) S X(t_f) + \int_{t_0}^{t_f} \{C_t + C_f f + C_r r(x, y)\} dt, \quad (7)$$

where  $X = [x \ y]^T$  is the state vector,  $S$  is the final state cost matrix,  $C_t$  is the cost coefficient of time,  $C_f$  is the cost coefficient of fuel,  $f$  is fuel flow rate,  $C_r$  is the cost coefficient of penalty areas, and  $r(x, y)$  is the penalty function. Using the chain rule of differentiation on the final state penalty cost, the cost function is rewritten as

$$J = \int_{t_0}^{t_f} [(SX(t))^T \dot{X}(t) + C_t + C_f f + C_r r(x,y)] dt \quad (8)$$

Pontryagin's Minimum Principle<sup>9</sup> is applied to determine the control input that minimizes the cost function. The heading angle,  $\theta$ , is the control available for aircraft during cruise. The Hamiltonian for this problem is defined as

$$H = (SX(t))^T \dot{X}(t) + C_t + C_f f + C_r r(x,y) + \lambda_x (V \cos \theta + u(x,y)) + \lambda_y (V \sin \theta + v(x,y)) + \lambda_m (-f) \quad (9)$$

where  $\lambda_x, \lambda_y$ , and  $\lambda_m$  are the co-state parameters. The study in Ref.16 determined the value of  $\lambda_m$  to be negligible during the cruise portion of flight for transport-class aircraft. If  $S$  is a diagonal matrix and  $s_x$  and  $s_y$  are the diagonal elements associated to the final position in  $x$  and  $y$  coordinates, the Hamiltonian for the reduced-order model is formulated as

$$H = s_x \dot{x} + s_y \dot{y} + C_t + C_f f + C_r r(x,y) + \lambda_x (V \cos \theta + u(x,y)) + \lambda_y (V \sin \theta + v(x,y)) = C_t + C_f f + C_r r(x,y) + (\lambda_x + s_x x)(V \cos \theta + u(x,y)) + (\lambda_y + s_y y)(V \sin \theta + v(x,y)). \quad (10)$$

For an extremum to exist, the optimal heading angle satisfies

$$\begin{aligned} \frac{\partial H}{\partial \theta} &= 0, & t_0 \leq t \leq t_f \\ \Rightarrow (\lambda_x + s_x x) \sin \theta &= (\lambda_y + s_y y) \cos \theta \\ \Rightarrow \tan \theta &= \frac{(\lambda_y + s_y y)}{(\lambda_x + s_x x)}, \end{aligned} \quad (11)$$

and the necessary conditions for optimality are

$$\begin{aligned} H^* &= \min\{H\}, & \text{in general} \\ H^* &= 0, & \text{free terminal time, } t_f. \end{aligned} \quad (12)$$

Solve Eqs. (10, 11) for the co-state parameters  $\lambda_x$  and  $\lambda_y$  when the Hamiltonian is zero to obtain

$$\lambda_x = \frac{-(C_t + C_f f + C_r r(x,y)) \cos \theta}{V + u(x,y) \cos \theta + v(x,y) \sin \theta} - s_x x \quad (13)$$

$$\lambda_y = \frac{-(C_t + C_f f + C_r r(x,y)) \sin \theta}{V + u(x,y) \cos \theta + v(x,y) \sin \theta} - s_y y. \quad (14)$$

The co-state equations are

$$\begin{aligned} \dot{\lambda}_x &= -\frac{\partial H}{\partial x} \Rightarrow \\ -\dot{\lambda}_x &= C_r \frac{\partial r(x,y)}{\partial x} + (\lambda_x + s_x x) \left( \frac{\partial u(x,y)}{\partial x} \right) \\ &+ s_x (V \cos \theta + u(x,y)) + (\lambda_y + s_y y) \left( \frac{\partial v(x,y)}{\partial x} \right) \end{aligned} \quad (15)$$

$$\begin{aligned} \dot{\lambda}_y &= -\frac{\partial H}{\partial y} \Rightarrow \\ -\dot{\lambda}_y &= C_r \frac{\partial r(x,y)}{\partial y} + (\lambda_x + s_x x) \left( \frac{\partial u(x,y)}{\partial y} \right) \\ &+ (\lambda_y + s_y y) \left( \frac{\partial v(x,y)}{\partial y} \right) + s_y (V \sin \theta + v(x,y)). \end{aligned} \quad (16)$$

Equations (11,15,16) are known as the Euler-Lagrange equations. As shown in Ref. 17, the dynamical equation for the optimal aircraft heading is governed by Eqs. (11-17), and the heading angle,  $\theta$ , is the solution to the differential equation

$$\begin{aligned} \dot{\theta} &= \frac{(V + u(x,y) \cos \theta + v(x,y) \sin \theta)}{(C_t + C_f f + C_r r(x,y))} \\ &\cdot (-C_r \sin \theta \frac{\partial r(x,y)}{\partial x} + C_r \cos \theta \frac{\partial r(x,y)}{\partial y}) \\ &+ \sin^2 \theta \left( \frac{\partial v(x,y)}{\partial x} \right) + \sin \theta \cos \theta \left( \frac{\partial u(x,y)}{\partial x} - \frac{\partial v(x,y)}{\partial y} \right) \\ &- \cos^2 \theta \left( \frac{\partial u(x,y)}{\partial y} \right). \end{aligned} \quad (17)$$

This equation reduces to the solution of Zermelo problem<sup>9</sup> when  $C_r = 0$ . Solving the equations (4,5,17) provides the optimal path. The initial heading angle at  $t_0$  must be picked correctly for a particular origin and destination pair. This study applies the shooting method in Ref. 18 to find the initial aircraft heading. The great circle heading at the origin can be used to initialize the shooting method.

### B. Aircraft Fuel Consumption Model

This study applies the fuel consumption model in Eurocontrol's Base of Aircraft Data Revision 3.6 (BADA)<sup>19</sup> to compute cruising aircraft fuel consumption. The following equation calculates fuel burn for aircraft during cruise

$$f = t \cdot SFC \cdot Th \quad (21)$$

where  $f$  is the fuel burn during cruise,  $t$  is elapsed time,  $Th$  is thrust, and  $SFC$  is the specific fuel consumption. At a given altitude and airspeed, the fuel flow is a constant. Thus, the factor  $C_t + C_f f$  in equation 17 is a constant and can be replaced by a single parameter  $C_k$ .

### C. Contrails as Penalty Areas

Persistent contrails are modeled using penalty functions as areas to be avoided by an aircraft to reduce the potential impact on climate. The penalty functions are used as a systematic way of generating aircraft trajectories that avoid the contrail formation areas by varying amount. The cost due to persistent contrails formation in the cost function is defined as

$$J_r = \int_{t_0}^{t_f} C_r r(x,y) dt.$$

The penalty function  $r(x,y)$  is the penalties that an aircraft can encounter along the flight trajectory from the origin to destination. In general, there are multiple regions in the en-route airspace that favor persistent contrails formation. The penalty can be determined by one of the following functions:

1. Radial penalty functions-

$$r(x,y) = \sum_i \frac{1}{d_i}, \text{ or} \quad (18)$$

$$r(x,y) = \sum_i \frac{1}{d_i^2}, \quad (19)$$

where  $d_i$  is distance between the aircraft and the center of  $i^{\text{th}}$  region that potentially form persistent contrails. The penalty function is set to zero if the aircraft is outside the penalty area.

2. Uniform penalty function-

$$r(x,y) = \begin{cases} \text{Constant} & \text{Aircraft in penalty area,} \\ 0 & \text{Otherwise.} \end{cases} \quad (20)$$

In this study, optimal trajectories will be generated using the penalty function defined in Eq. (19). In addition, there are many regions in the NAS that can potentially form persistent contrails. Some are far away from the aircraft and will not be encountered by the aircraft. Some are expected to be encountered, but the area is too large for aircraft to completely avoid. Identifying the right subset of contrails and avoiding the region by an appropriate level are important for policy makers to make operational decisions and trade-offs.

## IV. RESULTS

This section presents results based on applying the optimal trajectory algorithm to calculate an aircraft trajectory in the presence of winds that avoids regions of airspace that facilitate persistent contrails formation. The trajectory computations are conducted using traffic and atmospheric data in the continental United States for May 24, 2007. The data for wind speed and direction are obtained from RUC. The blue, green and magenta polygons in Fig. 2 depict the areas at 37,000 feet above sea level in the U.S. national airspace where

atmospheric conditions are favorable for persistent contrails formation at 6 a.m., 7a.m. and 8 a.m. EDT on May 24, 2007, respectively. The critical relative humidity and RHi values are computed using Eq. (1-3) with RHW values, pressure, and temperature data obtained from RUC. Figure 2 shows that the location, shape and size of potential contrail regions vary with time.

### A. Chicago (O'Hare International Airport) to Washington (Dulles International Airport)

The trajectory design in this example focuses on avoiding the potential contrails regions between Chicago and Washington D.C. At each altitude,  $C_r$  is varied from zero to a value where the optimal trajectory completely avoids the contrail region. The time for the wind optimal route, the time through contrail regions, the value of  $C_r$  to avoid contrails and the extra fuel consumption are computed at each altitude. This process is repeated at all six altitudes. Three optimal trajectories from Chicago O'Hare airport (ORD) to Washington Dulles airport (IAD) are shown in Fig. 3 for flights with cruising altitude equal to 37,000 feet. The cruising speed is assumed to be 420 nmi/hr (778 km/hr). The green arrows represent the wind directions, obtained from RUC, at 6 a.m. EDT on May 24, 2007. The arrow sizes are plotted in proportion to the wind magnitudes. The wind-optimal trajectory is generated using Eqs. (4, 5, 17) by setting  $C_r = 0$ . Two optimal trajectories in addition to the wind-optimal route are also plotted in Fig. 3. The areas favorable to persistent contrails formation are surrounded by the blue polygons. The polygon with a red cross is identified as a potential penalty area to the aircraft and the red cross is the center of penalty area. The position of penalty centers and aircraft position are used in Eq. (19) to calculate the distance and the penalty cost. In this example, the cost coefficient of time is chosen as  $C_k = 20$ . The cost coefficient of penalty  $C_r$  is equal to 0.5 and 2.0, respectively. Note that the penalty coefficient  $C_r$  is treated as a design parameter. The choice of this parameter is not unique and depends on the definition of the penalty function itself. The optimal route with  $C_r = 2.0$  completely avoids the contrail polygons near the departure airport. The optimal route with  $C_r = 0.5$  only partially avoids the polygons but is shorter. In this case, there is a trade-off between flying a shorter route with more persistent contrails formation versus flying a longer route with less persistent contrails formation. The performance of optimal trajectories is evaluated by investigating the total travel time and the time associated traveling through regions of persistent contrails formation.

Optimal aircraft trajectories are generated for six different altitudes between 29,000 feet and 39,000 feet. Figure 4 shows the results for the six wind-optimal trajectories. The sum of blue and red bars represents the

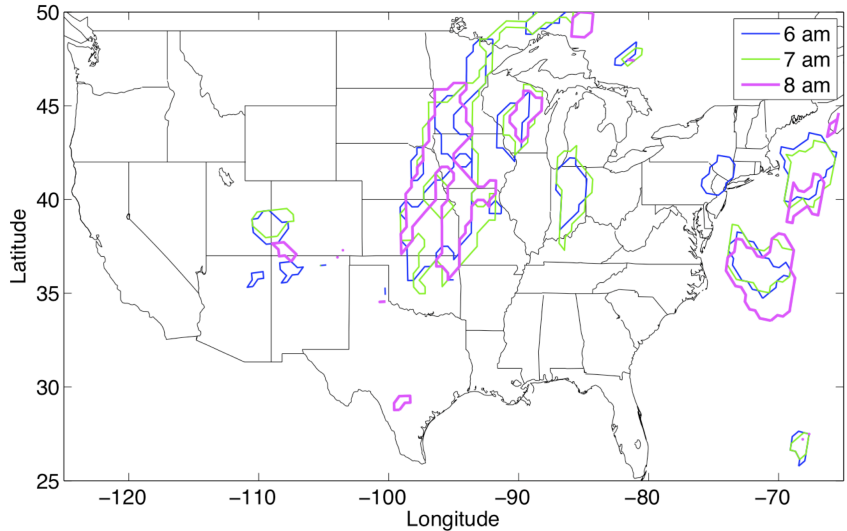


Figure 2. Regions of airspace at 37,000 feet where favorable to persistent contrails formation at 6 a.m., 7 a.m., and 8 a.m. on May 24, 2007.

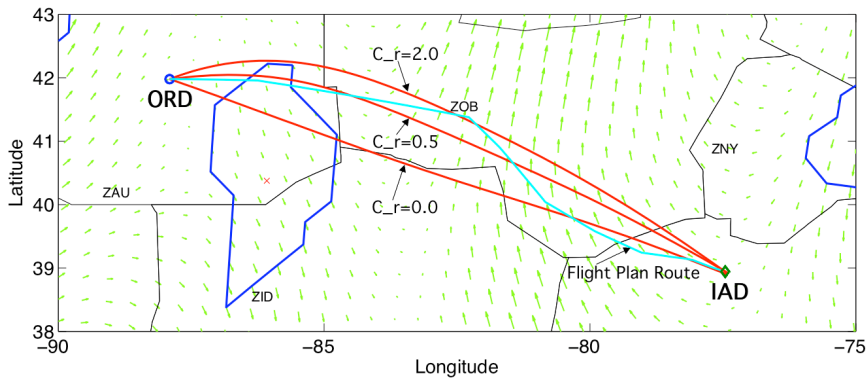


Figure 3. Optimal trajectories at 37,000 feet from ORD to IAD with different design parameters.

total travel time for each trajectory, and the red bar represents the amount of time that a flight travels inside the regions of airspace favorable to persistent contrails formation. The wind-optimal trajectories at 29,000 ft, 31,000 ft, 33,000 ft, and 35,000 ft do not intercept any region of airspace that facilitates persistent contrails formation. The flights at these cruising altitudes should fly the wind-optimal trajectories that minimize fuel burn and emissions. Flying wind optimal trajectories at 37,000 ft and 39,000 ft will potentially cause persistent contrails formation. Optimal contrails-avoidance trajectories at these altitudes are generated by increasing the value of  $C_r$  from 0 to 2 with increments equal to 0.1.

The green columns in Table 1 show the value of  $C_r$ , the total fuel consumption for the contrails-avoidance trajectory and the additional fuel burn compared to that of wind-optimal trajectory. The blue columns show the data for wind-optimal trajectories. Flying a contrails-avoidance trajectory requires 1.81% additional fuel burn at 37,000 feet and 39,000 feet, respectively,

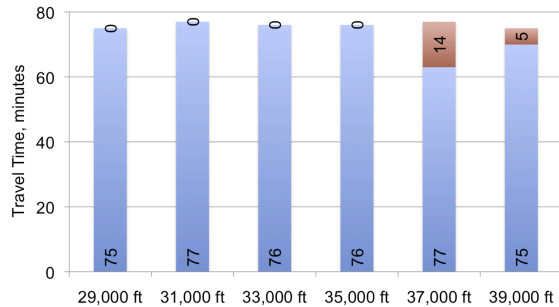


Figure 4. Travel time for the wind-optimal routes from ORD to IAD and length of periods favorable to persistent contrails formation at 6 different altitudes.

avoid potentially 14 minutes and 5 minutes of persistent contrails formation. More optimal trajectories can be calculated with various choice of  $C_r$ .

It is interesting to compare the optimization results with a typical aircraft trajectory at 37,000 feet, shown in cyan color in Fig. 3, flown from ORD and IAD. The typical trajectory takes 4 minutes longer and consumes an additional 145 Kg of fuel compared to the optimal

**Table 1. Wind-optimal trajectories (in blue) versus contrails-avoidance trajectories (in green) from ORD to IAD.**

Altitude (ft)	29,000	31,000	33,000	35,000	37,000	39,000	
$C_r$	0	0	0	0	0	2.0	0.6
Contrails (minute)	0	0	0	0	14.0	0	5
Fuel Burn (Kg)	3020	2978	2885	2814	2756	2806	2658

trajectory. However, the travel time through contrail regions is 5 minutes compared to the 14 minutes for the wind-optimal route.

*B. Optimal Trajectories for 12 City Pairs*

This section analyzes the wind-optimal and contrails-avoidance trajectories for 12 origin-destination pairs for a period of 24 hours starting from 6 a.m. EDT on May 24, 2007. The same city-pairs were used by the Federal Aviation Administration to assess the impact of implementation of Reduced Vertical Separation Minima (RVSM) on aircraft-related fuel burn and emissions<sup>20</sup>. This part of the study adapts the standard in RVSM and assumes that the cruising altitudes are between 29,000 and 41,000 feet. Figure 5 shows the wind-optimal trajectories for the eastbound flights at 37,000 feet at 6 a.m. EDT. Blue polygons depict the areas favorable to persistent contrails formation. The optimal aircraft trajectories are generated at the beginning of each hour on May 24, 2007 using hourly updated weather data from RUC. Six flight levels are considered for each direction of air traffic for each city pair. A group of 21 optimal aircraft trajectories are calculated for each flight level by increasing the value of  $C_r$  from 0 to 2 with increments equal to 0.1. The cost coefficient of time is chosen as  $C_t = 20$  for each case. The cruising true airspeed is assumed to be 420 nmi/hr. The fuel consumption for each aircraft trajectory is calculated using BADA formulas by assuming that the aircraft are short to

medium range jet airliners with medium weight. In each group, the additional fuel consumption of each optimal trajectory is obtained by comparing its fuel burned to that of its wind-optimal trajectory ( $C_r = 0$ ). The persistent contrails formation time associated to each trajectory is also recorded.

A total of six bins are defined such that the aircraft trajectories can be categorized based on their additional fuel consumption. The first bin contains the wind-optimal trajectory, which is the baseline for fuel use comparison and corresponds to trajectories that require no additional fuel consumption. The second bin contains aircraft trajectories consuming less than 2% additional fuel, the third bin contains those consuming between 2% to 4 % additional fuel, and etc. The sixth bin has trajectories that burn more than 8% of fuel. In each bin, the optimal trajectory that has least amount of persistent contrails formation time is selected to represent the bin. Note that there are six bins for each group of trajectories and six groups for each direction of air traffic every hour. The average persistent contrails formation time for the optimal trajectories are summarized in Table 2. The white column presents the average contrails formation time measured in minutes for the wind-optimal trajectories. The average is taken over six flight levels and a period of 24 hours for each direction. Flying wind-optimal routes on any of the six flight levels between Miami (MIA) and Newark, NY (EWR) or between Washington, DC (IAD) and MCO do not induce persistent contrails formation that day.

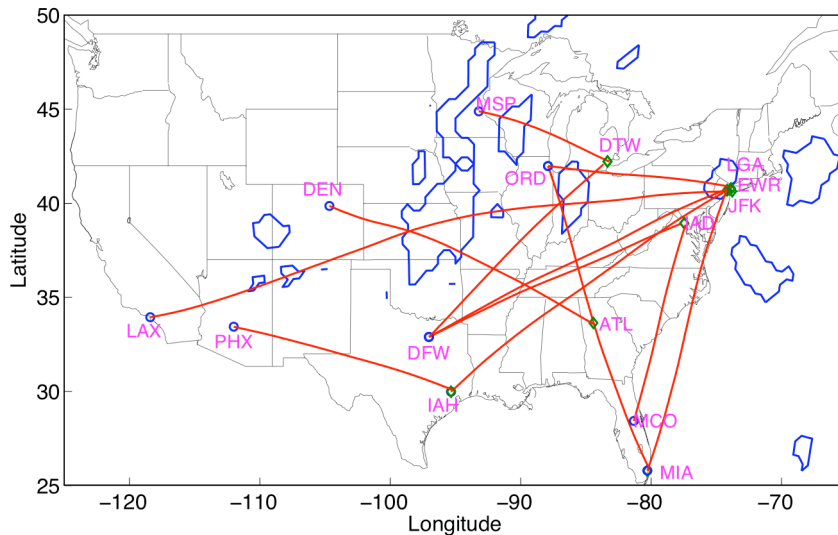


**Figure 5. The wind-optimal trajectories for the eastbound flights for 12 city pairs on 37,000 feet at 6 a.m. EDT on May 24, 2007.**

Table 2. Average persistent contrails formation time (minutes) for the optimal aircraft trajectories for the 12 cities on May 24, 2007.

City-pair	Maximum Additional Fuel Consumption (%)											
	0	2		4		6		8		8+		
LAX to JFK	7.8	3.8	1.6	2.8	0.4	2.5	0.1	2.0	0.0	0.2	0.0	
JFK to LAX	10.8	5.3	1.8	3.6	0.4	1.3	0.0	1.2	0.0	0.5	0.0	
ATL to DEN	8.1	5.5	3.4	4.4	0.8	3.6	0.0	3.0	0.0	1.8	0.0	
DEN to ATL	6.3	4.6	2.9	3.8	0.7	3.6	0.0	3.4	0.0	4.1	0.0	
DTW to DFW	2.4	1.6	0.4	1.1	0.0	1.0	0.0	0.8	0.0	0.5	0.0	
DFW to DTW	3.2	2.5	1.2	1.8	0.2	1.1	0.0	0.9	0.0	0.5	0.0	
PHX to IAH	2.2	1.7	1.6	1.6	0.1	1.4	0.0	1.4	0.0	1.3	0.0	
IAH to PHX	3.3	2.5	0.0	2.2	0.0	2.0	0.0	2.0	0.0	1.9	0.0	
DFW to LGA	1.5	1.1	0.6	0.7	0.1	0.6	0.0	0.5	0.0	0.4	0.0	
LGA to DFW	1.6	1.1	0.4	0.7	0.0	0.4	0.0	0.2	0.0	0.1	0.0	
DFW to IAD	1.3	0.8	0.4	0.6	0.2	0.5	0.0	0.5	0.0	0.3	0.0	
IAD to DFW	1.2	0.8	0.4	0.7	0.0	0.5	0.0	0.4	0.0	0.2	0.0	
ORD to LGA	0.9	0.5	0.3	0.4	0.1	0.3	0.0	0.3	0.0	0.3	0.0	
LGA to ORD	1.3	0.6	0.3	0.5	0.1	0.3	0.0	0.3	0.0	0.3	0.0	
MSP to DTW	0.7	0.5	0.3	0.5	0.2	0.3	0.0	0.3	0.0	0.2	0.0	
DTW to MSP	0.5	0.5	0.1	0.4	0.0	0.2	0.0	0.2	0.0	0.1	0.0	
IAH to EWR	0.8	0.6	0.1	0.5	0.0	0.5	0.0	0.4	0.0	0.3	0.0	
EWR to IAH	0.2	0.1	0.0	0.1	0.0	0.0	0.0	0.0	0.0	0.0	0.0	
ORD to MIA	0.4	0.1	0.1	11.3	0.0	9.8	0.0	8.8	0.0	3.1	0.0	
MIA to ORD	0.3	0.1	0.0	0.0	0.0	0.0	0.0	0.0	0.0	0.0	0.0	
MIA to EWR	0.0	0.0	0.0	0.0	0.0	0.0	0.0	0.0	0.0	0.0	0.0	
EWR to MIA	0.0	0.0	0.0	0.0	0.0	0.0	0.0	0.0	0.0	0.0	0.0	
IAD to MCO	0.0	0.0	0.0	0.0	0.0	0.0	0.0	0.0	0.0	0.0	0.0	
MCO to IAD	0.0	0.0	0.0	0.0	0.0	0.0	0.0	0.0	0.0	0.0	0.0	

The contrails formation time is less than a minute on average for the city pairs such as Minneapolis (MSP)-Detroit (DTW), Houston (IAH)-EWR, and Chicago (ORD)-MIA. The blue column presents the average contrails formation time for the optimal contrails-avoidance trajectories. These optimal trajectories consume different amounts of additional fuel at each bin or column. In general, the flights, which can afford more additional fuel burn, induce fewer contrails since they have more routes to choose from. The green column presents the average contrails formation time for the optimal contrails-avoidance trajectories on the optimized altitudes that produce least amount of contrails. The flights, which can select the flying altitudes, induce much fewer contrails given the same amount of extra fuel.

The data in Table 2 can be converted into actual amount of extra fuel consumed by various flights and then can be aggregated to produce a simplified total extra fuel consumption versus total minutes through the contrail regions for all the flights between the 12 city-pairs. This case is referred to as the baseline case. Figure 6 shows the curves with (green) and without (blue) altitude optimization. The figure shows, when altitude is optimized, a two percent increase in total fuel consumption can reduce the total travel times through contrail regions from 55 minutes to 16 minutes. Allowing further increase does not result in

proportionate reduction in contrail travel times. Without altitude optimization, the reduction in contrail travel times is small with increase in total fuel consumption. The data in Table 2 can be used to develop optimal fleet allocation and scheduling strategies to minimize the travel time through contrails.

## V. EFFECT OF UNCERTAINTIES

There are several uncertainties in developing trade-off between persistence contrail times and additional fuel flow. A major source of error is the relative humidity values used to generate the contrail regions. The relative humidity values are provided by RUC weather models. It has been observed that numerical weather models underestimate humidity in the upper-tropospheric regions<sup>21</sup>. NOAA has been improving the RUC models and the Rapid Refresh (RR) is the next-generation version of the system, planned to replace the current RUC by July-August 2011. Figure 7 shows relative humidity contours (top figure) using the RUC model and the corresponding contours (bottom figure) using the RR version of RUC. For a given latitude and longitude, the humidity values are different in the two versions and the humidity values are indicated by the vertical color bar. Further, the figure shows the regions where conditions are present for persistent contrail formation as regions enclosed by magenta color. Assuming RHw values in RUC models are

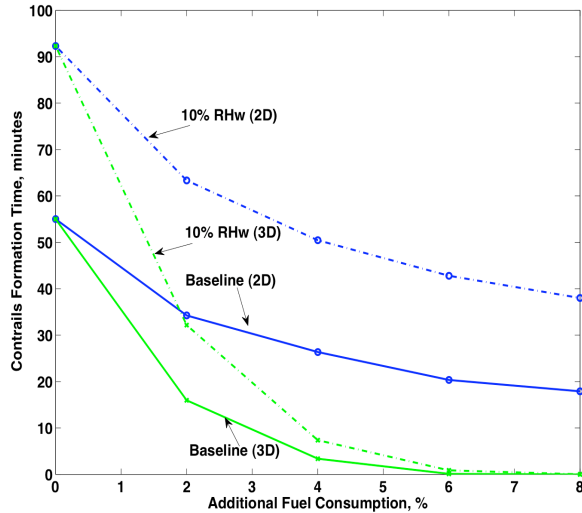


Figure 6. Trade-off curves between fuel consumption and contrail avoidance.

underestimated, the trade-off curves computations for city-pairs are repeated by increasing the RHw values by 10%. The trade-off curves with 10% additional humidity is shown in (dotted lines) Figure 6. The amount of time wind optimal routes go through persistent contrail regions increases to 92 minutes from 55 minutes due to the changes in the contrail formation areas. As in the baseline case, use of altitude optimization results in a significant reduction of travel time through contrail regions from 92 minutes to 32 minutes by using only 2% extra fuel. Similarly, for horizontal maneuvers only, the decrease in travel time through contrail regions is small with extra fuel consumption. Although, the actual trade-off curves are different the trend observed in the baseline is maintained even in the presence of uncertainties in the contrail formation regions due to uncertainties of relative humidity values in weather forecast models.

## VI. CONCLUSIONS

This study develops an algorithm to calculate wind-optimal trajectories for aircraft while avoiding the regions of airspace that facilitate persistent contrails formation. The optimal trajectories are developed by solving a non-linear optimal control problem with path constraints. The operational strategies investigated in this study for minimizing aviation impacts on climate change include flying wind-optimal routes, avoiding complete or partial persistent contrails formation and altering cruising altitudes.

The trade-off between persistent contrails formation and additional fuel consumption is investigated for 12 city-pairs in the continental United States. When both horizontal maneuvers and altitude are optimized, a 2% increase in total fuel consumption can reduce the total

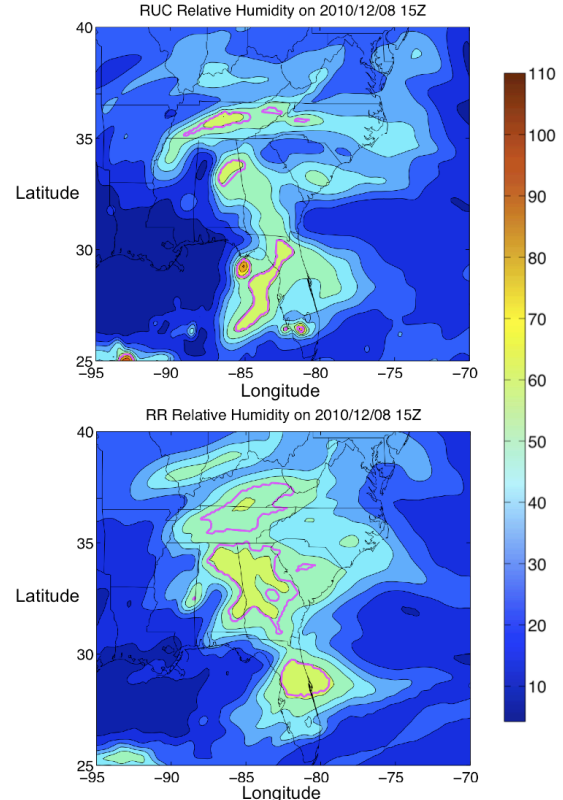


Figure 7. Relative humidity with respect to water (RHw) and contrail regions from RUC (top) and the RR version (bottom).

travel times through contrail regions by more than 70%. Allowing a further increase in fuel consumption does not seem to result in a proportionate decrease in contrail travel times. Without altitude optimization, the reduction in contrail travel times is small with an increase in total fuel consumption. The trade-off curves maintain similar behavior even in the presence of uncertainties in modeling contrail regions.

The results in this paper were based on traffic for a single day and used the same type of aircraft on all routes. The results can be modified using the complete traffic and weather data for extended periods of time to get a better understanding of the complex relation between fuel efficiency and contrail reduction. CO<sub>2</sub> emissions are directly proportional to the amount of fuel used during a flight. The cost function in the trajectory optimization has to be modified to include the effect of NO<sub>x</sub> emissions as the amount of emission for a unit amount of fuel varies with altitude and ambient conditions. An important product resulting from this research is the development of an integrated capability combining traffic flow management concepts with both CO<sub>2</sub> and non-CO<sub>2</sub> emissions. Policy and better understanding of the tradeoff between emissions and the contrail minutes and impact on the climate through

the use of RF functions need to be developed to fully utilize this new capability. Alternatively, the optimization results can be used as inputs to global climate modeling tools like the FAA's Aviation Environmental Portfolio Management Tool for Impacts<sup>22</sup>.

## REFERENCES

- [1] Schumann, U., 1996: On Conditions for Contrail Formation from Aircraft Exhausts. *Meteor. Z.*, N. F. 5, 3–22.
- [2] Duda, D.P., Minnis, P., Costulis, P.K., and Palikonda, R. "CONUS Contrail Frequency Estimated from RUC and Flight Track Data," European Conference on Aviation, Atmosphere, and Climate, Friedrichshafen at Lake Constance, Germany, June-July, 2003.
- [3] Waitz, I., Townsend, J., Cutcher-Gershenfeld, J., Greitzer, E., and Kerrebrock, J. Report to the United States Congress: Aviation and the Environment, A National Vision, Framework for Goals and Recommended Actions. Partnership for Air Transportation Noise and Emissions Reduction, MIT, Cambridge, MA, 2004.
- [4] Klima, K., "Assessment of a Global Contrail Modeling Method and Operational Strategies for Contrail Mitigation," M.S. Thesis, MIT, 2005.
- [5] Mannstein, H., Spichtinger, P., and Gierens, K., "A Note on How to Avoid Contrail Cirrus," *Transportation Research Part D*, Vol. 10, No. 5, 2005, pp. 421-426.
- [6] Campbell S.E., Neogi, N. A., and Bragg, M. B., "An Optimal Strategy for Persistent Contrail Avoidance," AIAA 2008-6515, AIAA Guidance, Navigation, and Control Conference, Honolulu, Hawaii, 2008.
- [7] Gierens K., Lim, L. and Eleftheratos K. "A Review of Various Strategies for Contrail Avoidance," *The Open Atmosphere Science Journal*, 2, 1-7, 2008.
- [8] Naidu, D. S., and Calise, A. J., "Singular Perturbations and Time Scales in Guidance and Control of Aerospace Systems: A Survey," *AIAA Journal of Guidance, Control and Dynamics*, Vol. 24, No. 6, pp. 1057-1078, Nov.-Dec., 2001.
- [9] Bryson, A. E., and Ho, Y. C., *Applied Optimal Control*, Taylor and Francis, Levittown, PA, 1975.
- [10] Appleman, H., 1953: The Formation of Exhaust Condensation Trails by Jet Aircraft. *Bull. Amer. Meteor. Soc.*, Vol. 34, 14–20.
- [11] Ponater, M., Marquart, S., and Sausen, R., "Contrails in a Comprehensive Global Climate Model: Parameterization and Radiative Forcing Results," *Journal of Geophysical Research*, 107(D13), 2002.
- [12] Degrand J. Q., Carleton, A. M., Travis D. J., and Lamb, P. J., "A Satellite-Based Climate Description of Jet Aircraft Contrails and Associations with Atmospheric Conditions, 1977-79," *Journal of Applied Meteorology*, Vol. 39, pp. 1434-1459.
- [13] Palikonda R., Minnis P., Duda, D.P., and Mannstein H., "Contrail Coverage Derived from 2001 AVHRR Data Over the Continental United States of America and Surrounding Areas," *Meteorologische Zeitschrift*, Vol. 14, No. 4, 525-536, August 2005.
- [14] Alduchov, O. A., and R.E. Eskridge, "Improved Magnus form Approximation of Saturation Vapor Pressure," *Journal of Applied Meteorology*, Vol. 35, 601-609.
- [15] Vian, J. L., and Moore, J. R., "Trajectory Optimization with risk Minimization for Military Aircraft," *J. Guidance*, Vol. 12, No., 3, May-June 1989.
- [16] Burrows, J. W., "Fuel-Optimal Aircraft Trajectories with Fixed Arrival Times," *AIAA Journal of Guidance, Control, and Dynamics*, Vol. 6, Jan.-Feb. 1983, pp. 14-19.
- [17] Press, William H., Teukolsky, Saul A., Vetterling, William T., and Flannery, Brian P., *Numerical Recipes in C: The Art of Scientific Computing*, 2nd ed., Cambridge University Press, Cambridge, England, 1992, Chapter 17.
- [18] Sridhar, B., Ng, Hok K., and Chen, Neil Y., "Aircraft Trajectory Optimization and Contrails Avoidance in the Presence of Winds," ATIO Conference, September 2010, Fort Worth, TX.
- [19] Eurocontrol Experimental Center (EEC). "User Manual for the Base of Aircraft Data (BADA), Revision 3.6." EEC Note No. 10/04. Project ACE-C-E2. September 2004.
- [20] CDM/DRVSM Work Group Report, "Benefit Analysis and Report for Domestic Reduced Vertical Separation Minimum (DRVSM)," FAA Air Traffic Organization System Operations Services, September 2005.
- [21] Duda, D. P., Palikonda, R. and Minnis, P., "Relating Observations of Contrail Persistence to Numerical Weather Analysis Output," *Atmos. Chem. Phys.*, Vol. 9, 1357-1364, 2009.
- [22] ICAO Committee on Aviation Environmental Protection, Aviation Environmental Portfolio Management Tool (APMT) prototype, TG2-Meeting, Tucson, AZ, February 2006.

## AUTHORS' BIOGRAPHIES

**Dr. Banavar Sridhar** worked at Systems Control, Inc., Palo Alto, Ca and Lockheed Palo Alto Research Center before joining NASA Ames Research Center in 1986. He was recently appointed as NASA Senior Scientist for Air Transportation Systems. His research interests are in the application of modeling and optimization techniques to aerospace systems. Dr. Sridhar received the 2004 IEEE Control System Technology Award for his contributions to the development of modeling and simulation techniques. He led the development of traffic flow management software, Future ATM Concepts Evaluation Tool (FACET), which received the NASA Software of the Year Award in 2006. He is a Fellow of the IEEE and the AIAA.

**Dr. Hok K. Ng** is a senior software engineer at University of California, Santa Cruz. He specializes in algorithm development in traffic flow management. He has worked for the past three years on Aviation related researches and applications. He earned his Ph.D. degree in Mechanical and Aerospace Engineering from University of California, Los Angeles in 2005.

**Dr. Neil Y. Chen** Dr. Neil Chen is an aerospace research engineer in the Aviation Systems Division at NASA Ames Research Center. He received his Ph.D. degree in mechanical and aerospace engineering from University of California, Los Angeles, in 2001. He has been working in the area of air traffic management since 2006. His current research interests include traffic flow management and aviation induced environmental impact.

**Mr. Florian Linke** received a diploma in aeronautical engineering from the RWTH Aachen University in 2007 and is currently doing his Ph.D. at the Hamburg University of Technology (TUHH). Since 2008 he works at the German Aerospace Center (DLR) in the Air Transportation System institute in Hamburg as head of the department of Air Traffic Infrastructure and Processes. Mr. Linke is specialized in Flight Dynamics and Control as well as Rotorcraft Aerodynamics. He has several years of experience in Air Traffic Management and focuses on environmental issues and interactions in the Air Transportation System.